Nanoscale

Accepted Manuscript

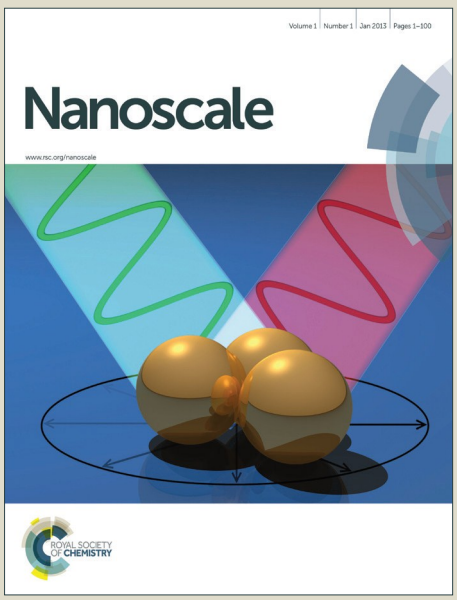

ROYAL SOCIETY OF CHEMISTRY

www.rsc.org/nanoscale

Ultra-Durable Rotary Micromotors Assembled from Nanoentities by Electric Fields

*Jianhe Guo[1], Kwanoh Kim[2], Kin Wai Lei[1], and D. L. Fan[1, 2] **

[1] Materials Science and Engineering Program, the University of Texas at Austin, Austin, TX 78712, USA
[2] Department of Mechanical Engineering, the University of Texas at Austin, Austin, TX 78712, USA

*Correspondence can be addressed to: dfan@austin.utexas.edu

Abstract

Recently, we reported an innovative type of micromotors consisting of nanowires as rotors and patterned Au/Ni/Cr nanodisks as bearings. The dimensions of micromotors were less than 1 μm, and could continuously rotate for 15 hours over 240,000 cycles. To understand the limitation of their lifetime, we systematically investigated the rotation dynamics by analytical modeling and determined the time-dependent torques and forces involved in the rotation. From the forces and torques, the extent of wear of micromotors was successfully derived, which well agreed with the experimental characterizations. The results also proved that frictional force linearly increases with the loading in such rotary nanodevices operating in suspension, consistent with the prediction of the non-adhesive multi-asperity friction theory. With these understandings, we enhanced the design of micromotors and achieved an operation lifetime of 80 hours and over 1.1 million total rotation cycles. This research, shining new light on the frictional mechanism of recently reported nanowire micromotor with demonstration of the *most* durable rotary nanomechanical devices of similar dimensions to the best of our knowledge, can be inspiring for innovative design of future nanomechanical devices with ultralong lifetime for practical applications.

Keywords: micromotors, NEMS, electric tweezers, nanorobotics, nanomagnetism

Introduction

Rotary micromotors, which can convert diverse input energy sources to mechanical rotary motions, are a type of devices critical for further advancing nanoelectromechanical systems (NEMS) devices.[1-3] Various approaches have been explored to rotate nanoentities, including nanospheres, nanowires, synthetic or rolled-up nanotubes, helical, crossed, and gear-shaped structures by using chemical/biochemical propulsion or external physical fields (light, magnetic fields, electrical fields, or ultrasonic waves).[3-17] Especially, magnetic field manipulation is one of the most well established techniques. Spiral-shaped magnetic nanostructures and flexible nanowires could be transported by converting the axial rotational motions into translations in the long direction.[9, 18] Freely rotating magnetic nanowires could move along close-by walls and convey polymer microbeads, microorganisms, and even human blood cells to various locations.[19, 20] Even more, rotation of rolled-up magnetic nanotubes with sharp tips were used for drilling soft matters, e.g., porcine liver tissue as a model system.[11]

However, with the aforediscussed methods, it remains extremely difficult to use the as-synthesized micro/nanoparticles as rotary micro/nanomotors that can stably operate at fixed positions with high speeds, which is essential for effectively transmitting forces and torques as well as coupling micro/nanomotors with other devices.[12, 13, 19, 21-23] Recently, we reported an innovative type of micromotors that can be efficiently assembled and stably rotated at designated locations with ultrahigh speeds by utilizing nanoscale building blocks with nanowires as rotors and patterned nanomagnets as bearings. The employed field-assisted assembling strategy, based on the electric tweezers, greatly reduced the difficulties in fabricating rotary NEMS devices compared with traditional top-down fabrication technologies.[24, 25] The micromotors also exhibited

enhanced performance and could continuously rotate for 15 hours over 240,000 cycles,[26] well above the common operational time of minutes of other rotary NEMS of similar dimensions.[19, 21, 23] The micromotor can rotate to a speed of at least 18,000 rpm. As a promising application in biomedical fields, the micromotors demonstrated biochemical release at tunable rates with their precisely controllable rotation speeds.[26, 27] Despite the high performance and demonstrated applications, the inability to withstand a prolonged contact between the rotors and bearings due to the interfacial friction and wear is still a major obstacle for applications of the micromotors in practice. Also note that tribology issues, such as friction and wear, are surface phenomena, which play a dominating role in determining the lifetime of rotary NEMS due to the miniaturized dimensions.[28, 29] Therefore, it is highly desirable to understand the evolving nanoscale interactions among different components of micromotors, the rotation dynamics, as well as their correlations with the interfacial wear of the micromotors during the long-term operation, which collectively determine the device lifetime.

In this work, we systematically investigated the rotation characteristics including the time-dependent speeds, forces, and torques during the long-term operation of the micromotors. From analytical modeling, the evolvement of the nanoscale interactions was determined, which well predicted the extent of wear of the devices. Our results also proved the linear dependence between friction forces and load in this nano-mechanical system, agreeing with the results of the non-adhesive multi-asperity friction theory. Moreover, with these understandings, we employed a highly wear-resistant material (Ti) as the contact layer between the rotors and bearings in place of Au in the previous design, which improved the lifetime of micromotors to at least 80 hours and over 1.1 million

rotation cycles in total. To the best of our knowledge, the demonstrated lifetime and operating cycles are the best among rotary micromotors of similar dimensions. This research is the first attempt in a newly developed rotary NEMS and the results could be inspiring for designing future rotary nano-mechanical devices with ultra-long lifetime.

Results and discussions

Design, fabrication, and assembling of micromotors

The micromotors with multisegment nanowires anchored on patterned magnetic nanobearings were efficiently assembled and actuated by the electric tweezers [Fig. 1(a)].[25, 26] Unlike our previous research, the building blocks of our micromotors, including nanowires and patterned nanomagnets were both obtained by large-scale bottom-up synthesis, which could be scaled up for mass production. The fabrication details are given in the supporting information.

In brief, the nanowires were synthesized with controlled diameter and length by electrodeposition into polycarbonate nanoporous templates in a three-electrode setup[30,31] [Fig. 1(b)]. A large number of magnetic bearings of multi-layer thin film stacks, e.g., Au/Ni/Cr, were batch fabricated on the quadruple microelectrodes by the colloidal lithography technique, different from previous research [supporting information and Fig. S1]. The as-obtained magnetic bearings were monodispersed in both diameters and thicknesses, similar to those fabricated by the conventional electron-beam lithography, while the productivity was significantly improved [Fig. 1(c)].

With the prepared nanoentities as building blocks for the rotors and bearings, the micromotors were assembled by the software-controlled electric tweezers, a recently developed nanomanipulation technique that could align and transport longitudinal

nanoentities with a resolution less than 300 nm.[24, 31] The Au/Ni/Au nanowires suspended in deionized (DI) water were transported in both the X and Y directions to the vicinity of the magnetic bearings. The transport velocity and alignment orientation could be separately controlled by the applied DC and AC voltages, respectively.[24] When a nanowire was approaching a nanomagnet, the strong magnetic attraction between the Ni segment in the nanowire and the Ni layer in the magnetic bearing swiftly assembled the nanowire rotor atop of the magnetic bearing and formed a micromotor. By applying four AC electric voltages with sequential 90° phase shift on the quadruple microelectrodes, the micromotor could be compelled to rotate with controlled angle, speed, and orientation [Fig. 1(d)].

Rotation dynamics during long-term operation

We investigated the evolvement of the nanoscale interactions between the rotors and bearings during long-term rotation of two types of micromotors with different contact materials on top of the bearings, while both of them had similar dimensions for all the components. The first type of micromotors had Au of 500 nm in diameter as the contact layer between the rotor [165 nm-diameter Au (1.8 um)/Ni (500 nm)/Au (1.8 um) nanowire] and bearing [nanodisk made of a thin film stack of Au (60 nm)/Ni (80 nm)/Cr (6 nm), 500 nm in diameter] [Fig. 2(a)]. It could rotate for as long as 22.6 hours (Supplementary Video S1). The rotation speed oscillated sinusoidally with a primary periodicity of 360° [Fig. 2(c)]. During the 22-hour rotation, the average rotation speed decreased monotonically with time while the speed oscillation amplitude increased till the nanorotor was finally arrested on the bearing [Fig. 2(a) and (c)]. We investigated the evolvement of the torques involved in the rotation, which governs the observed rotation

dynamics, device wear, and lifetime.[25, 26, 32, 33] In brief, five torques could be identified in the system. The magnetic forces that anchor the nanorotors on the bearings result in angle dependent magnetic (τ_M) and frictional torques (τ_f). The micromotors are rotated by the electric torque (τ_e) induced by the external *E*-field. The electric torque depends on the relative polarization of the nanowire in the water suspension and is proportional to the square of the *E*-field intensity (E^2) and thus the square of the AC voltage (V^2) ($\tau_e \sim V^2$).[34] Noteworthy, the external *E*-field also induces electric polarization between the metallic rotor and bearing and results in a non-negligible induced torque ($\tau_{e'}$), which is also proportional to V^2. Also, we need to consider the viscous torque (τ_η) from the water medium given by:[35]

$$\tau_\eta = a\omega = \frac{1}{3}\omega\pi\eta l^3 \frac{N^3-N}{N^3\left[\ln\left(\frac{l}{Nr}\right)+0.5\right]}\ [\mathrm{N\cdot m}]\ , \quad (1)$$

where ω is rotation speed, η is the viscosity of DI water, a is a constant for a nanorotor with a radius of *r*, length of *l*, and the number of segments *N*. The segments are not separated by the composition and set as $N = 2$ in this study for calculation purpose only. The aforementioned five torques balance in a micromotor and can be given as[26] $\tau_\eta = \tau_e + \tau_{e'} + \tau_M + \tau_f$. It can be rewritten as $a\omega = bV^2 + cV^2 + \tau_M + \tau_f$, where *b* and *c* are constants and the sum of *b* and *c* can be readily determined from the slopes of ω–V^2 for the rotation of a nanowire rotor assembled on a bearing in Fig. 2(b). To calculate the magnetic forces and torques, we employed a simplified magnetic dipole-dipole model with the horizontal magnetic moments of the nanowire and bearing taken as m_1 and m_2, respectively.[36] The analytical solution of the magnetic torque and force can be readily determined as below:[26]

$$\tau_M(r, \Theta, m_1, m_2) = \mu_0(m_1 m_2 \sin\Theta)/(4\pi x^3), \quad (2)$$

$$F_M(r, \Theta, m_1, m_2) = 3\mu_0(m_1 m_2 \cos\Theta)/(4\pi x^4) + f, \quad (3)$$

where μ_0 is the magnetic permittivity of vacuum, Θ and x are the angle and the separation distance between m_1 and m_2, respectively, and f is the force due to the non-angle-dependent vertical magnetic moments and other factors. Theoretical research indicates that the frictional force (F_f) in nanoscale contacts should linearly or sub-linearly increase with the load depending on the nature of the contact.[37-41] Therefore, the frictional torque (τ_f) due to the angle-dependent magnetic force (F_M) should have a dominating factor proportional to $(\cos\Theta)^z$. Experimentally, we found the rotation speed of micromotors showed a strong 360° ($z = 1$) periodicity as given in the Fourier transform in Fig. 2(c). Also note that micromotors did not have clear periodicities related to $z < 1$, (e.g., $z = 2/3$, sublinear dependence, 480° periodicity for a non-adhesive single-asperity contact according to theoretical study[38]), although a low-level 180° periodicity (corresponds to $z = 2$) was found and could be attributed to axial rolling of the nanorotor due to small transverse magnetic moments possibly existing in the nanowires.[42] This suggests that the frictional force that contributes to the fluctuation of the rotation speed of the micromotors should have a 360° periodicity. Then $z = 1$. Therefore, the frictional force (F_f) should be linearly proportional to the loading force. In such a case, according to theoretical study, the nature of the contact in our micromotors is multi-asperity and non-adhesive.[41] In the multi-asperity model, a contact between objects consists of multiple much smaller contacting points. If they are non-adhesive, the actual contact area is proportional to the loading force. [41] Also the frictional force is proportional to the actual contact areas. Therefore the frictional force linearly depends on the loading force in the non-adhesive multi-asperity mode. We note that the nature of contacts in our micromotors is consistent

with that of the non-adhesive multi-asperity conditions. The surfaces of neither the rotors nor the bearings are perfectly smooth and the size of the contacts is at least 500 nm in diameter. The rotors and bearings can hardly form a single asperity contacting point when having relative motions. Multiple much smaller contacts are expected between the rotors and bearings. Moreover, the adhesion in the contacts is also low due to the natural lubrication effect of liquid when operating in an aqueous solution. As a result, the sum of the magnetic and frictional torques can be readily written as, $\tau_M + \tau_f = d\sin(\theta - \theta_M) + e\cos(\theta - \theta_M) + g$, where d, e, and g are constants, θ and θ_M are the angular positions of magnetic orientation of the nanowire and the nanobearing, respectively, and $\Theta = \theta - \theta_M$. Therefore, we can obtain:

$$a\omega = d\sin(\theta - \theta_M) + e\cos(\theta - \theta_M) + g + (b + c)V^2. \quad (4)$$

Now, by fitting the oscillating speed of the micromotor during the long-term rotation according to Eq. (4), the time dependent coefficients of d, e, and g can be readily determined [details in the supporting information]. The values of d and e are amplitudes of the angle-dependent magnetic and frictional torques, respectively as shown in Fig. 3(a). We note that there are high frequency noises in addition to the strong 360° periodicity of the rotation speed [Fig. 2(c)], which can be attributed to factors such as Brownie motions, uncontrolled surfaces roughness and imperfectness of the nanowires and magnetic nanobearing, as well as instant liquid agitations. These factors can not be easily modelled and not considered in the fitting equation (4). They contributed to the slight differences of the fitting curves from the experimentally determined rotation speed in Fig. 2(c). However, the strong 360° periodicity of the rotation speed can be just attributed to the magnetic and the resulted frictional torques in the micromotors, and make the method

feasible. As shown in Fig. 3(a), both the amplitude of the magnetic torque (*d*) and frictional torque (*e*) monotonically increase during the 22-hour rotation. Our calculation shows that the levels of the magnetic and frictional forces are $1.0 – 2.2\times10^{-12}$ and $0.9 – 1.5\times10^{-13}$ N, respectively. Even with such low interfacial forces, significant wear of the bearing was observed after 22-hour rotation as shown in the scanning electron microscopy (SEM) images [Fig. 3(b)]. It was found that the Au spacing layer had an obvious thickness reduction and deformation. Especially, the wear on the bottom right corner of the magnetic bearing was more severe than the other regions, which could be attributed to the center of rotation of the nanorotor located close to that region of the magnetic bearing, i.e., the bottom right corner [Fig. 3(b)]. The nanowire rotors did not show clearly observable wear (Fig. S2), which can be attributed to the fact that Ni (Element Vickers hardness: 638 MPa) is much harder than Au (Element Vickers hardness: 216 MPa).[43] The detailed analysis of the extent of wear on the rotors and bearings in terms of the rotation center, materials, fabrication method and the mechanical hardness is provided in the supporting information. According to Eqs. (2 – 4), it can be readily understood that the increase of the values of *d* and *e* during micromotor rotation [Fig. 3(a)] is due to the wear and thickness reduction of the Au separation layer because the magnetic and frictional torques increase with the decrease of the separation distance (x) between the two magnetic moments in the rotor and bearing, with a dependence of $1/x^3$ and $1/x^4$, respectively. Note that the separation distance (x) is calculated from the middle of the Ni segment of the nanowire to the center of the magnetic Ni layer in the bearing. From Eq. (4) and the time-dependent amplitude of the magnetic torque (*d*) in Fig. 3(a), we can readily determine the separation distance (x) and thus the thickness of the Au

layer during the rotation of the micromotor as shown in Fig 3(c). The final thickness of the Au layer was determined as 29 nm as shown in Fig. 3(c), which well agreed with the average thickness of ~ 26 nm in the most worn region obtained by the Atomic Force Microscopy (AFM) characterization [Fig. S3]. The consistent calculation and experimental results well support our modeling. Moreover, we found the amplitude of the magnetic load and the frictional torque obtained from experiments in Fig. 3(a) linearly depend on each other as shown in the log-log plot in Fig. 3(d). This provides another proof of our understanding and modeling of the system, where the frictional torque linearly increases with the load. Three micromotors of this type were tested, which continuously rotated for 16.4, 21.1, and 22.6 hours, respectively. All of these motors showed the same decreasing trends in speed due to the wear of the bearings. The tested lifetime in the range of 16.4 to 22.6 hours demonstrated the fairly good repeatability of our micromotor devices.

With the characterization and understanding of the wearing issues of the bearings after long-term rotation, the design of the micromotors was modified for improved durability by replacing the Au layer (Element Vickers hardness: 216 MPa) with the much harder Ti (Element Vickers hardness: 970 MPa)[43] as the top layer of the bearing. The new micromotors had a similar geometry shown in Fig. 4(a) with a 500 nm-diameter contact area between the rotors and bearings. The rotors are Au/Ni/Au nanowires of 165 nm in diameter and 4.1 μm in length [Au (1.8 μm)/Ni (500 nm)/Au (1.8 μm)], and the bearings are 500 nm diameter nanodisks made of the thin film stacks of Ti (60 nm)/Cr (6 nm)/Ni (80 nm)/Cr (6 nm). The additional Cr layer between Ti and Ni was used to enhance the adhesion of the films. We rotated micromotors on Ti protected bearing both clockwise

and counterclockwise. The rotation continued for 80 hours over 1.1 million cycles in total [Fig. 4(a) and Video S2]. The speed during the 80 hour rotation just decreased less than 10% from the original value [Fig. 4(a)]. Both the duration and the number of cycles were around 4 times of those of the Au-spaced micromotors with a similar geometry. As far as we know, this is a new record in both duration and number of cycles among reported rotary motors made from synthesized nanoparticles. From the rotation speed, we determined the time-dependent magnetic and frictional torques. Similar to that found in the Au-supported micromotor, the magnetic torque monotonically increases with time [inset of Fig. 4(b)]. The frictional force goes up with the magnetic torque with a power-law dependence of 0.994±0.036 [Fig. 4(c)], which further confirm the consistence with the non-adhesive multi-asperity friction theory we discussed previously. After 80 hours rotation, the micromotor was dissembled, which could be possibly due to a small bubble generated in the sealed chamber because of water evaporation or some other unknown reasons that require further investigation. Neither the magnetic bearing nor nanowire rotor was obviously worn after such a long-term rotation [Fig. 4(d) and S4]. The SEM images does not show obvious thickness reduction of the Ti layer on top of the magnetic bearing, which is consistent with the prediction of only 4.68 nm decrease in thickness derived from the time-dependent magnetic torques with our modeling [Fig. 4(b) and (d)]. From the above analysis, we can estimate the wear rate of the motor as 0.0585 nm/hour. This value can assist to estimate the lifetime of the micromotors as 632 hours (26.3 days) given the final thickness of 29 nm of the separation layers (Au) before the nanowire rotor is arrested due to the increased magnetic/frictional forces between the rotor and bearing [Fig. 3(c)]. Alternatively, by directly extrapolating the thickness v.s. time curve for the Ti

micromotor in Fig. 4(b) and Fig. S5 in the supporting information, the lifetime of such micromotors can be estimated as 1088 hours (45.3 days). Both estimation methods suggest the lifetime is ultralong, i.e. at least hundreds of hours. Note that the estimations have simple assumptions that the frictional coefficients of Au and Ti are the same, the wear rate is constant, and the nanowire rotors do not wear. A more accurate lifetime can be calculated if knowing the wear rate of the nanowire rotor with consideration of the reduced magnetic force and thus frictional force during its wear. The results indicate that the replacement of the spacer layer with Ti can indeed increase the lifetime of micromotors significantly. The micromotor could potentially rotate with a much longer life time than 80 hours.

Conclusion

In summary, this work reported micromotors assembled from mass-produced nanoentities rotated up to 80 hours for over 1.1 million cycles. With an analytical model of the rotation dynamics, we determined the evolving magnetic and frictional torques during the long-term rotation, from which the extent of wear of the nanobearing could be calculated. The modeling results well agreed with the experimental characterizations, which supported the feasibility of our analysis of the micromotors. It also suggested that the contacts between the rotors and bearings in our micromotors had a multi-asperity and non-adhesive nature. Employing mechanically hard materials between the contact of rotors and bearings, we significantly reduced the wear of the micromotors and improved the operation lifetime, which is critical for practical applications of this new type of micromotors demonstrated in tunable biochemical release.[26, 27] The results presented in

this research could inspire new designs for MEMS/NEMS devices with ultra-long lifetime.

Acknowledgement

This research was supported by the National Science Foundation (CAREER Award CMMI 1150767), Welch Foundation (Grant No. F-1734), NIH (9R42ES024023-02) in part, and Research Grant from the Vice President Office for Research at UT-Austin.

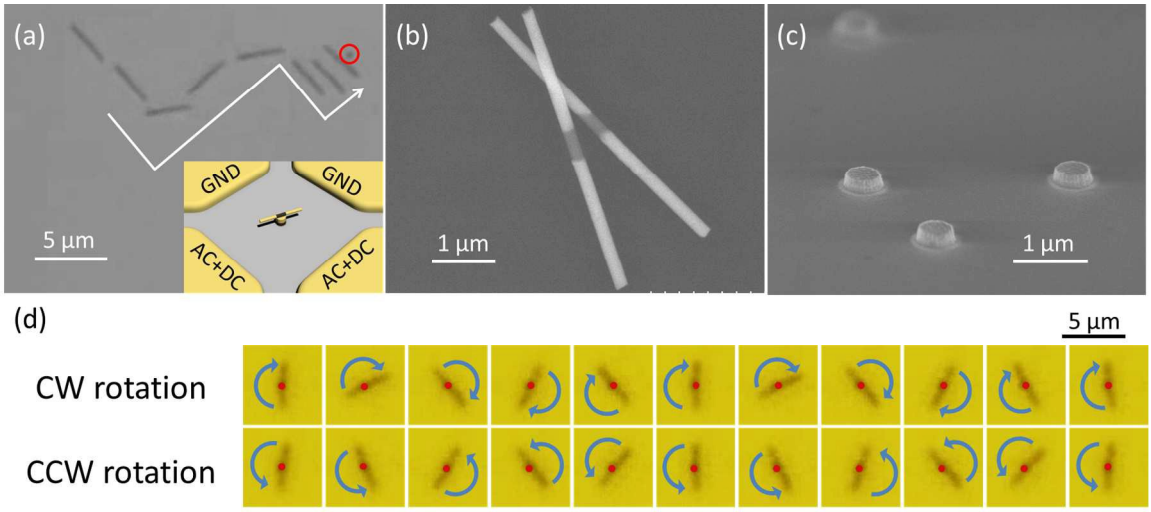

Figure 1. (a) Overlapped snapshots of an Au/Ni/Au nanowire transported and assembled on a magnetic bearing (highlighted by the red circle) by the electric tweezers. Inset: Illustration of the microchip for the electric tweezers. (b – c) Scanning electron microscopy (SEM) images of (b) Au/Ni/Au nanowires and (c) magnetic bearings. (d) Sequential optical images of a micromotor rotating clockwise (CW) and counterclockwise (CCW) every 60 ms. The positions of the bearing are highlighted by red dots.

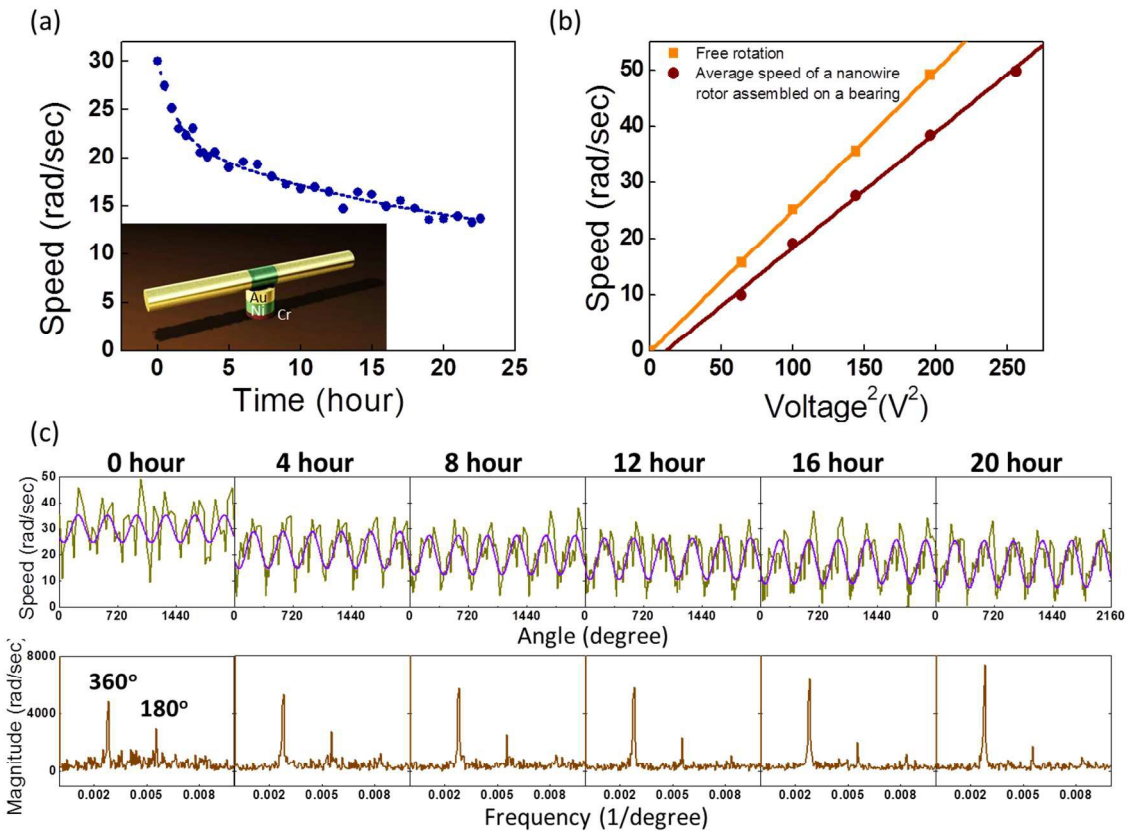

Figure 2. Micromotor with a 500 nm-diameter Au bearing area rotated for 22.6 hours. [rotor: Au(1.8 μm)/Ni(500 nm)/Au(1.8 μm) nanowires, 165nm in diameter; bearing: magnetic disks made of tri-layer Au (60 nm)/Ni (80 nm)/Cr (6 nm), 500nm in diameter] (a) Rotation speed versus time, insert: schematic diagram of the micromotor (non-proportional dimensions); (b) average rotation speed versus applied voltage^2 (V^2) for nanowire rotors (wine red) and free suspending nanowires (orange); (c) Rotation speed versus angular position at different time and the corresponding Fourier transform showing the primary periodicity.

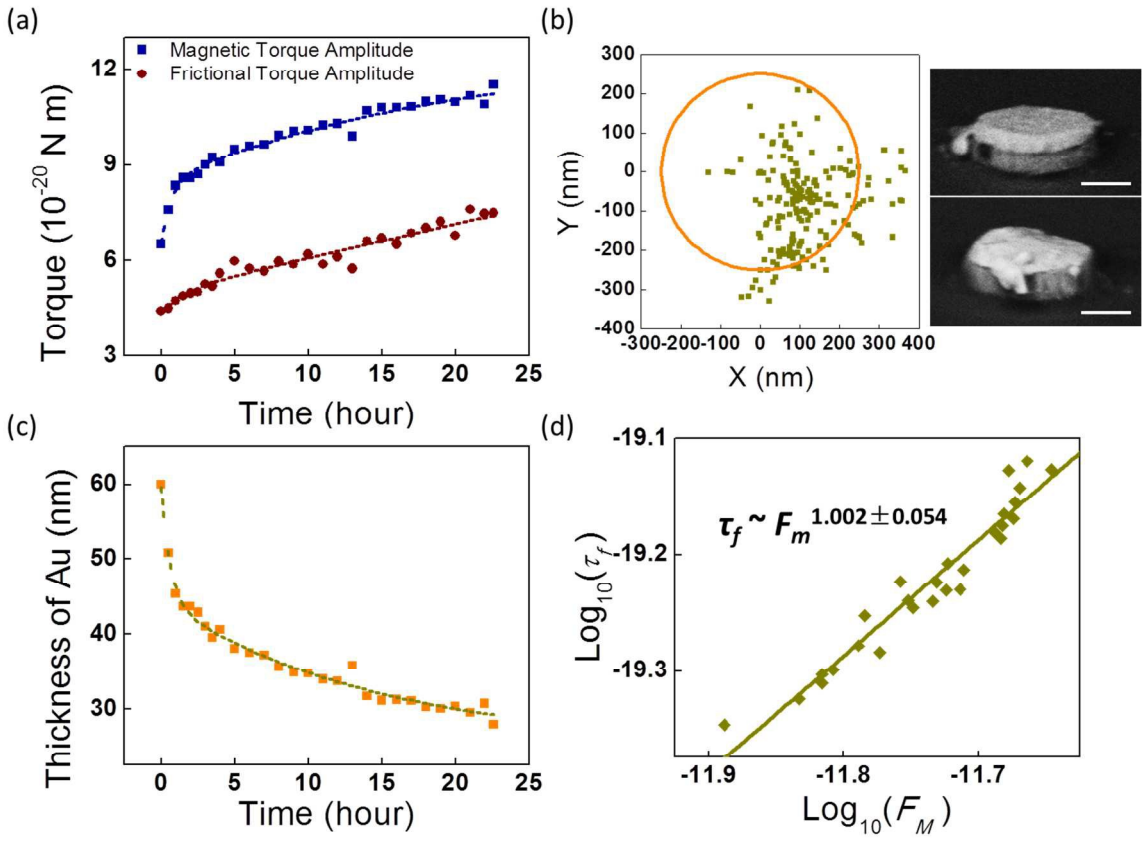

Figure 3. (a) Amplitude of the magnetic and frictional torques versus time during the 22.6-hour rotation; (b) left: instant center of rotation of the micromotor primarily formed at the bottom right corner of the magnetic nanobearing (at 22.6 hours); right: SEM images of an as-made nanobearing (top) and the nanobearing after supporting rotation for 22.6 hours (bottom). The scale bar is 250 nm; (c) time dependent change of the thickness of the Au spacer layer determined from the evolving magnetic torque during the rotation; (d) Log-log plot of the amplitude of frictional torque versus that of the magnetic force showing a power dependence of ~1 (slope of the plot).

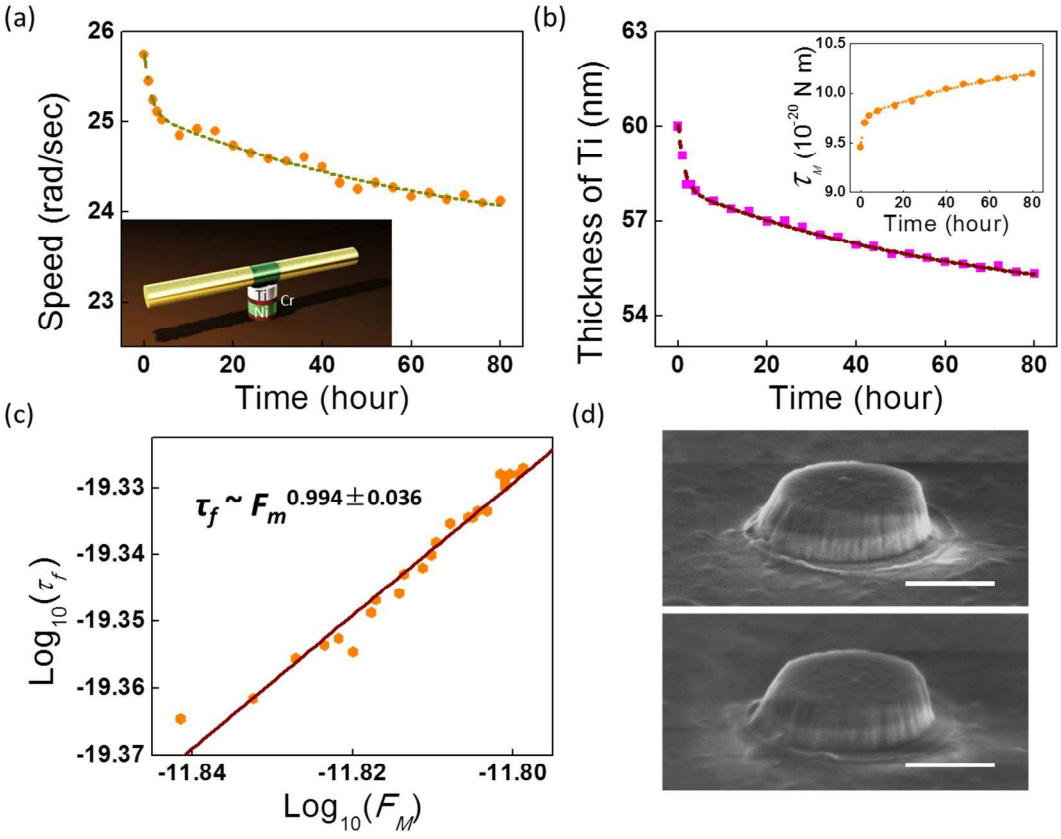

Figure 4. Micromotor made of a Ti topped bearing of 500 nm in diameter rotated for 80 hours, clockwise (1-6 hour) and counterclockwise (7-80 hour) [rotor: Au(1.8 μm)/Ni(500 nm)/Au(1.8 μm), 165 nm in diameter; bearing: 500 nm in diameter, thin-film stack of Ti (60 nm)/Cr (6 nm)/Ni (80 nm)/Cr (6 nm)]: (a) rotation velocity versus time, insert: schematic diagram of the micromotor (non-proportional dimensions); (b) time dependent change of the thickness of the Ti spacing layer determined from the magnetic torque during rotation of the micromotor, insert: amplitude of the angle-dependent magnetic torque versus time; (c) Log-log plot of the amplitude of frictional torque versus that of the magnetic force showing a power dependence of ~1 (slope of the plot). (d) SEM images of an as-made magnet bearing (top) and magnet bearing after 80-hour rotation. Scale bar is 250 nm.

References:

1. J. W. Judy, *Smart Mater. Struct.*, 2001, **10**, 1115-1134.
2. G. A. Ozin, I. Manners, S. Fournier-Bidoz and A. Arsenault, *Adv. Mater.*, 2005, **17**, 3011-3018.
3. M. Guix, C. C. Mayorga-Martinez and A. Merkoci, *Chem. Rev.*, 2014, **114**, 6285-6322.
4. S. Fournier-Bidoz, A. C. Arsenault, I. Manners and G. A. Ozin, *Chem. Commun.*, 2005, DOI: 10.1039/b414896g, 441-443.
5. Y. P. He, J. S. Wu and Y. P. Zhao, *Nano Lett.*, 2007, **7**, 1369-1375.
6. A. L. Balk, L. O. Mair, P. P. Mathai, P. N. Patrone, W. Wang, S. Ahmed, T. E. Mallouk, J. A. Liddle and S. M. Stavis, *ACS Nano*, 2014, **8**, 8300-8309.
7. M. Liu, T. Zentgraf, Y. M. Liu, G. Bartal and X. Zhang, *Nat. Nanotechnol.*, 2010, **5**, 570-573.
8. D. J. Bell, S. Leutenegger, K. M. Hammar, L. X. Dong and B. J. Nelson, presented in the Proceedings of the 2007 IEEE International Conference on Robotics and Automation, Rome, Italy, 2007, 1128-1133.
9. W. Gao, S. Sattayasamitsathit, K. M. Manesh, D. Weihs and J. Wang, *J. Am. Chem. Soc.*, 2010, **132**, 14403-14405.
10. L. M. Tong, V. D. Miljkovic and M. Kall, *Nano Lett.*, 2010, **10**, 268-273.
11. W. Xi, A. A. Solovev, A. N. Ananth, D. H. Gracias, S. Sanchez and O. G. Schmidt, *Nanoscale*, 2013, **5**, 1294-1297.
12. E. J. Garcia and J. J. Sniegowski, *Sens. Actuator A-Phys.*, 1995, **48**, 203-214.
13. R. K. Soong, G. D. Bachand, H. P. Neves, A. G. Olkhovets, H. G. Craighead and C. D. Montemagno, *Science*, 2000, **290**, 1555-1558.
14. D. L. Fan, F. Q. Zhu, R. C. Cammarata and C. L. Chien, *Phys. Rev. Lett.*, 2005, **94**, 4.
15. D. L. Fan, F. Q. Zhu, X. B. Xu, R. C. Cammarata and C. L. Chien, *Proc. Natl. Acad. Sci. U. S. A.*, 2012, **109**, 9309-9313.
16. K. Kim, J. H. Guo, X. B. Xu and D. L. Fan, *Small*, 2015.
17. J. G. Gibbs and P. Fischer, *Chem. Commun.*, 2015, **51**, 4192-4195.
18. A. Ghosh and P. Fischer, *Nano Lett.*, 2009, **9**, 2243-2245.
19. L. G. Frechette, S. F. Nagle, R. Ghodssi, S. D. Umans, M. A. Schmidt and J. H. Lang, presented in the 14th IEEE International Conference on Micro Electro Mechanical Systems, Interlaken, Swizerland, 2001, 290-293.
20. L. Zhang, T. Petit, K. E. Peyer and B. J. Nelson, *Nanomed.-Nanotechnol. Biol. Med.*, 2012, **8**, 1074-1080.
21. A. M. Fennimore, T. D. Yuzvinsky, W. Q. Han, M. S. Fuhrer, J. Cumings and A. Zettl, *Nature*, 2003, **424**, 408-410.
22. L. G. Frechette, S. A. Jacobson, K. S. Breuer, F. F. Ehrich, R. Ghodssi, R. Khanna, C. W. Wong, X. Zhang, M. A. Schmidt and A. H. Epstein, *J. Microelectromech. Syst.*, 2005, **14**, 141-152.
23. N. Ghalichechian, A. Modafe, M. I. Beyaz and R. Ghodssi, *J. Microelectromech. Syst.*, 2008, **17**, 632-642.
24. D. L. Fan, R. C. Cammarata and C. L. Chien, *Appl. Phys. Lett.*, 2008, **92**, 3.
25. K. Kim, F. Q. Zhu and D. L. Fan, *ACS Nano*, 2013, **7**, 3476-3483.
26. K. Kim, X. B. Xu, J. H. Guo and D. L. Fan, *Nat. Commun.*, 2014, **5**, 9.

27. X. B. Xu, K. Kim and D. L. Fan, *Angew. Chem.-Int. Edit.*, 2015, **54**, 2525-2529.
28. E. Riedo, J. Chevrier, F. Comin and H. Brune, *Surf. Sci.*, 2001, **477**, 25-34.
29. J. A. Williams and H. R. Le, *J. Phys. D-Appl. Phys.*, 2006, **39**, R201-R214.
30. T. M. Whitney, J. S. Jiang, P. C. Searson and C. L. Chien, *Science*, 1993, **261**, 1316-1319.
31. D. L. Fan, F. Q. Zhu, R. C. Cammarata and C. L. Chien, *Nano Today*, 2011, **6**, 339-354.
32. B. Bhushan, *Microelectron. Eng.*, 2007, **84**, 387-412.
33. B. Bhushan, *Tribology Issues and Opportunities in MEMS*, Kluwer Academic Publishers, Dordrecht, 1998.
34. T. B. Jones, *Electromechanics of Particles*, Cambridge University Press, New York, 2005.
35. K. Keshoju, H. Xing and L. Sun, *Appl. Phys. Lett.*, 2007, **91**, 3.
36. J. M. D. Coey, *Magnetism and Magnetic Materials*, Cambridge University Press, Dublin, 2010.
37. G. Amontons, *Mem. Acad. R. A*, 1699, 257–282.
38. H. Hertz, *J. Reine Angew. Math.*, 1881, **92**, 156.
39. D. Maugis, *J. Colloid Interface Sci.*, 1992, **150**, 243-269.
40. J. P. Gao, W. D. Luedtke, D. Gourdon, M. Ruths, J. N. Israelachvili and U. Landman, *J. Phys. Chem. B*, 2004, **108**, 3410-3425.
41. Y. F. Mo, K. T. Turner and I. Szlufarska, *Nature*, 2009, **457**, 1116-1119.
42. K. Kim, J. H. Guo, X. B. Xu and D. L. Fan, *ACS Nano*, 2015, **9**, 548-554.
43. G. V. Samsonov, *Handbook of the physicochemical properties of the elements*, IFI-Plenum, New York, 1968.